



Sequential morphological changes in follow-up CT of pulmonary mucormycosis

Ji Yung Choo, Chang Min Park, Hyun-Ju Lee, Chang Hyun Lee, Jin Mo Goo, Jung-Gi Im

PURPOSE

We aimed to describe the computed tomography (CT) features of pulmonary mucormycosis including sequential changes between follow-ups.

MATERIALS AND METHODS

Between June 2001 and May 2011, five patients (three males and two females; median age, 43 years; age range, 13–73 years) who had been pathologically diagnosed with pulmonary mucormycosis constituted our study population. Their clinical and CT features including sequential changes over follow-ups were evaluated retrospectively.

RESULTS

All patients were immunocompromised due to either hematologic diseases (n=3), diabetes mellitus (n=1), or steroid administration for autoimmune hepatitis (n=1). All patients had symptoms such as fever (n=5), tachycardia (n=1), or pleuritic chest pain (n=1) on admission. Regarding the clinical outcome after treatment, one patient died, and the remaining four recovered from the disease. In terms of initial CT features, the morphologies of pulmonary mucormycosis included a single mass (n=3), consolidation (n=1), or multiple masses (n=1). There were seven pulmonary lesions in total, 3–7 cm in size, which showed a CT halo sign (n=3), reversed-halo sign (n=2), or air-fluid levels (n=2). On follow-up CTs, the lesions of all patients contained necrosis. All three patients with a mass or masses with a CT halo sign on initial CT had a decreased surrounding halo followed by central necrosis, and the lesions gradually decreased in size on recovery.

CONCLUSION

Pulmonary mucormycosis usually manifests as a mass or masses with a halo or reversed-halo sign on the initial CT scan followed by a decreased extent of surrounding ground-glass opacities with the development of internal necrosis during follow-up.

Mucormycosis infection caused by fungi of the class *Zygomycetes*, most commonly the order *Mucorales* (1), is serious and often fatal clinically, typically in immunocompromised patients such as those with diabetes mellitus (DM), hematologic malignancies, or those that have undergone transplantation. Clinically, this infection has been reported to manifest as various distinct syndromes including rhinocerebral, pulmonary, abdominopelvic, and cutaneous forms, as well as disseminated mucormycosis (2–5).

Pulmonary mucormycosis is the second most common manifestation of this disease, accounting for more than 30% of all reported cases (3). It involves the lung parenchyma and airways, causing thrombosis of pulmonary vessels due to fungal angioinvasion and leading to pulmonary parenchymal necrosis. Correct diagnosis and prompt management of pulmonary mucormycosis is critical as it is often fatal (4). To date, however, few articles have reported the imaging findings of pulmonary mucormycosis (3, 6, 7). According to these reports, this disease may exhibit diverse morphologies such as consolidation, masses with a halo sign or a reversed-halo sign, necrotic or cavitory consolidation with an air-crescent sign, or solitary/multiple nodules and masses.

Yet, to our knowledge, there have been no radiological reports detailing the sequential computed tomography (CT) changes of pulmonary mucormycosis during follow-up after anti-fungal treatment. This information may be crucial, as recognition of the sequential changes on CT can help clinicians make the proper diagnosis, monitor the disease status, and predict the prognosis of affected patients. Therefore, the purpose of this study was to describe the CT features of pulmonary mucormycosis, including its sequential changes during and after treatment.

Materials and methods

Study subjects

Our Institutional Review Board approved this retrospective study, and the requirement for informed consent was waived. From June 2001 to May 2011, the data of seven patients (five males and two females; median age, 47 years; age range, 13–73 years) who had been diagnosed with pulmonary mucormycosis based on pathological examinations were retrieved from the electronic medical database of our institution. Among them, two patients were excluded: one patient who did not undergo follow-up imaging and another who had endobronchial mucormycosis without a pulmonary parenchymal lesion. The remaining five patients (three males and two females; median age, 43 years; age range, 13–73 years) had undergone chest CT and chest radiographs prior to the pathological diagnosis and had sequential follow-up images available;

From the Department of Radiology (J.Y.C., C.M.P. ✉ cmpark@radiol.snu.ac.kr, H.J.L., C.H.L., J.M.G. J.G.I.) Seoul National University College of Medicine, and Institute of Radiation Medicine, Seoul National University Medical Research Center, Seoul, Korea; the Department of Radiology (J.Y.C.), Korea University Ansan Hospital, Ansan, Korea.

Received 27 June 2013; revision requested 15 May 2013; revision received 25 June 2013; accepted 27 June 2013.

Published online 13 September 2013.
DOI 10.5152/dir.2013.13183

these constituted the study population (Table 1). The pathologic diagnosis of pulmonary mucormycosis was made via percutaneous needle biopsy (n=3), open lung biopsy (n=1), or lobectomy (n=1). There was no evidence of any coexisting infections in the pathological examinations or laboratory tests.

We retrospectively reviewed the clinical and laboratory findings of the five patients using the hospital electronic medical records, including age and gender, underlying systemic diseases such as malignancies, DM, hematologic diseases, history of organ transplantation or neutropenia, clinical symptoms including fever, tachycardia, and chest pain, initial laboratory data such as the white blood cell count, neutrophil count, biochemical analysis of C-reactive protein or erythrocyte sedimentation rate, cultures of blood, urine, sputum, and serum analysis of galactomannan, the time interval between initial symptoms and CT scan, type of treatment, and clinical outcome.

Image acquisition and analysis

All patients underwent chest radiographs and CTs on presentation at the emergency department or the outpatient clinic of our hospital. As for follow-up radiologic examinations, four patients underwent CT examinations with an interval of 2 to 52 days (median, 7 days): two follow-up CTs in three

patients, and one follow-up CT in one. The remaining patient underwent only follow-up chest radiographs.

Chest radiographs were obtained using digital radiographic equipment (TDR4600-F80, Gold Mountain Medial systems, Seoul, Korea) and a standardized technique: 110 kVp, 2 mAs, and a 180 cm film-focus distance for posteroanterior views. CT images were obtained using several CT scanners (MX-8000 [n=2], Brilliance-64 [n=3] [Philips Medical Systems, Best, The Netherlands], Sensation-16 [n=4] [Siemens Medical Systems, Erlangen, Germany], and Lightspeed Ultra [n=3] [GE Medical Systems, Milwaukee, Wisconsin, USA]). CT scanning parameters were as follows: detector collimation, 0.75–2.5 mm; table speed, 20–24 mm/s; slice thickness, 1.0–5 mm; reconstruction interval, 1.0–5.0 mm; 170–220 effective mAs; 120 kVp; and 512×512 matrix. Intravenous contrast medium was used for all CT scans.

All chest radiographs and chest CT images were evaluated jointly by two thoracic radiologists (C.M.P. and J.M.G. with 13 and 21 years of experience in thoracic CT interpretation), who reached their conclusions by consensus. Each chest radiograph and CT was assessed for lesion size, quantity, location and extent (lobar or multilobar), presence of the CT halo sign, and internal characteristics (presence of a reversed-halo, low attenuation,

or air-fluid level), as well as for associated findings such as mediastinal lymphadenopathy, pleural effusion or a CT halo sign. CT findings were interpreted using factors proposed by the Fleischner Society Nomenclature Committee; the CT halo sign was designated when there was ground-glass opacity (GGO) surrounding a nodule or mass and the reversed-halo sign was designated when a focal rounded area of GGO was surrounded by a complete ring of consolidation (8).

To assess lesion changes over follow-ups, sequential follow-up CT images were analyzed for each patient. The time interval, pattern change, increase or decrease in extent, and distribution of the lesions over follow-ups were investigated by comparing follow-up CTs with those conducted prior to treatment.

Results

Clinical and laboratory characteristics of pulmonary mucormycosis

Clinical and laboratory features of patients with pulmonary mucormycosis are summarized in Table 1. All patients had underlying systemic diseases, such as myelodysplastic syndrome (n=1), aplastic anemia (n=1), lymphoblastic leukemia (n=1), DM (n=1) or long-term use of immunosuppressants due to autoimmune hepatitis (n=1). All patients had symptoms, including fever (n=5), tachycardia (n=1), and

Table 1. Demographics of patients with pulmonary mucormycosis

Case number	Gender	Age (years)	Initial symptom	Underlying diseases	Interval between initial symptom and CT scan (days)	Laboratory finding			Treatment	Clinical outcome
						WBC (μL)	ANC (μL)	CRP (mg/dL) or ESR (mm/hour)		
1	Male	47	Fever, tachycardia	Myelodysplastic syndrome, BMT	0	11 800	718	CRP, 16.28	Lobectomy after antifungal therapy	Death
2	Male	43	Fever	Aplastic anemia	5	320	90	CRP, 23.61	Antifungal therapy	Survive
3	Male	22	Fever	T-lymphoblastic leukemia	12	70	0	Not available	Lobectomy after antifungal therapy	Survive
4	Female	13	Fever	Long term use of steroid due to autoimmune hepatitis	7	2690	38.7	ESR, 23	Antifungal therapy	Survive
5	Female	73	Pleuritic chest pain, fever	Diabetes mellitus, congestive heart failure	30	19 750	3893	ESR, 77	Antifungal therapy	Survive

ANC, absolute neutrophil count; BMT, bone marrow transplantation; CRP, C-reactive protein; CT, computed tomography; ESR, erythrocyte sedimentation rate; WBC, white blood cell. Galactomannan test was negative in all patients.

Table 2. Initial CT findings of pulmonary mucormycosis

Case number	Lesion size ^a (cm)	Number of lesions	Location	Extent	Mass/consolidation	Presence of CT halo sign	Internal characteristics
1	5.3/3.4	Multiple	Bilateral lower lobes	Multilobar	Masses	-	Reversed halo
2	3.4	Solitary	Right upper lobe	Segmental	Mass	+	Reversed halo
3	3.2	Solitary	Right lower lobe	Segmental	Mass	+	Low attenuation
4	6.7/5	Multiple	Bilateral lower lobes	Multilobar	Consolidations	-	Air-fluid levels in all lesions
5	7	Solitary	Right middle lobe	Segmental	Mass	+	Low attenuation

^aLesion size indicates the longest diameter of the largest lesion if multiple.

pleuritic chest pain (n=1). For treatment of pulmonary mucormycosis, all patients received anti-fungal therapy, and two patients eventually underwent lobectomy. Regarding post-treatment clinical outcomes, one patient died, and the remaining four patients survived.

Initial CT features and sequential morphological changes during follow-up

All patients underwent baseline CTs on the day of admission, and antifungal medication was initiated. Their initial CT features are summarized in Table 2. On initial CT examinations, pulmonary mucormycosis manifested as a solitary mass (n=3), multiple masses (n=1) or consolidation (n=1). There were seven pulmonary lesions in total, 3–7 cm in size, which had a CT halo sign (n=3), reversed-halo sign (n=2), or air-fluid levels (n=2) on initial CT. Follow-up CTs were performed two days to three months following the initial CT.

The clinical course and sequential morphological changes over follow-ups are summarized in Fig. 1. In all five patients, lesion size increased early during follow-up; however, three survivors who did not undergo lobectomy finally demonstrated a decrease in the size of the lesions. With regard to the morphologic changes during follow-up, the lesions in all patients had peripheral enhancement and central low attenuating necrosis on contrast-enhanced CT images. In one patient, the mass had the reversed-halo sign on initial CT and subsequent central necrosis (Fig. 2). In addition, three patients with a mass or masses with the CT halo sign on initial CT had a decreased surrounding halo, followed by central necrosis (Figs. 3, 4). The remaining patient with bilateral consolidations eventually showed an

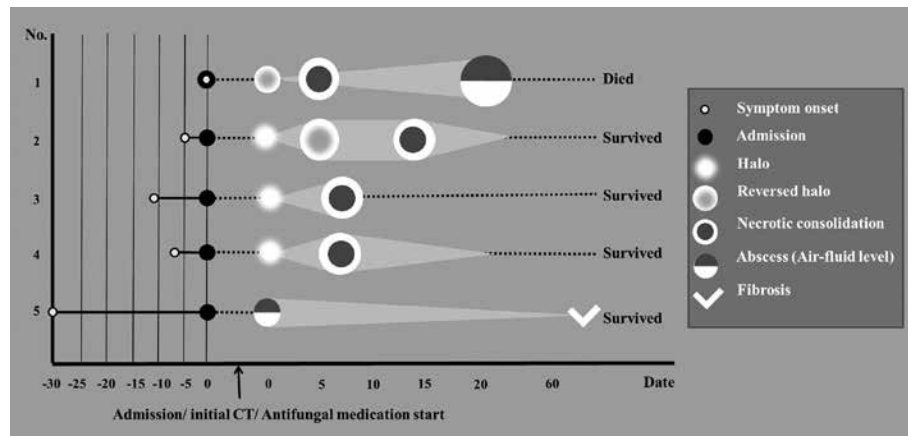


Figure 1. The brief clinical course and morphological changes during follow-up in five patients. All patients underwent initial CT on the day of admission and started antifungal medication. Although not all cases demonstrated the same morphological features simultaneously, most tended to show consistent sequential morphological changes over follow-ups. Note that the light gray triangle or quadrangle behind the round figure represents the size change of the lesions over follow-ups. Three patients (cases 2, 4, and 5) survived and their lesions were partially resolved on follow-up chest radiographs. The patient of case 3 was transferred to an outside hospital with clinical improvement. However, the follow-up chest radiographs of this patient could not be evaluated.

air-fluid level on follow-up. Other ancillary findings, such as pleural effusion or lymphadenopathy, were not present on initial CT; however, pleural effusion occurred in two patients during follow-up. There were no substantial differences between the CT morphological changes of hematologic and non-hematologic patients. The size changes in the lesions based on follow-up chest radiographs and CTs are depicted in Fig. 1.

Discussion

In our study, three of five patients (60%) had a mass or masses with the CT halo sign on initial CT. A halo around a mass on CT indicates pulmonary mucormycosis, which tends to invade pulmonary blood vessels causing pulmonary thrombosis and infarction (9–11). Jamadar et al. (6) also showed that six out of eight (75%)

mucormycosis lesions demonstrated the CT halo sign. In addition, two of the five patients (40%) in our study had the reversed-halo sign. Histologically, the central GGO area represents inflamed lung parenchyma with relative preservation of alveolar spaces. The peripheral radiopaque portion consists of dense and homogeneous intra-alveolar cellular infiltrates (12). Chung et al. (7) reported that the presence of the reversed-halo sign suggests pulmonary mucormycosis when invasive fungal infection is suspected. In immunocompromised patients, the presence of the reversed-halo sign on initial or follow-up CT may indicate pulmonary mucormycosis rather than invasive aspergillosis (7). However, the reversed-halo sign is not specific for pulmonary mucormycosis. We believe that it may be challenging to differen-



Figure 2. a–c. (Case 1) Pulmonary mucormycosis manifesting as masses with the “reversed-halo” sign in a 47-year-old male patient with myelodysplastic syndrome. Chest CT taken at admission (a) shows masses with the “reversed-halo” sign in both lower lobes. Internal cavitary changes are evident within the masses. Two days later, a CT image taken during percutaneous needle biopsy (b) shows masses with thick walled cavitations surrounded by growing ground-glass opacities. Although the patient was put on antifungal agents, these masses grew and showed more extensive cavitary changes with air-fluid level on the follow-up CT taken 19 days later (c). He underwent right lower lobectomy for further treatment; however, the patient died.

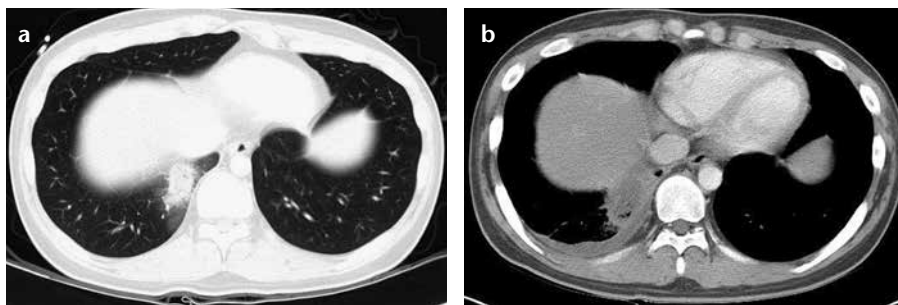


Figure 3. a, b. (Case 3) Pulmonary mucormycosis appearing as a mass with the halo sign on CT in a 22-year-old male patient with T-lymphoblastic leukemia. Chest CT taken at admission (a) shows a 3.5 cm mass with a halo on CT in the right lower lobe of the lung. Follow-up CT taken six days later (b) demonstrates the increased size of the mass with internal low attenuating necrosis. A small amount of right pleural effusion is noted.

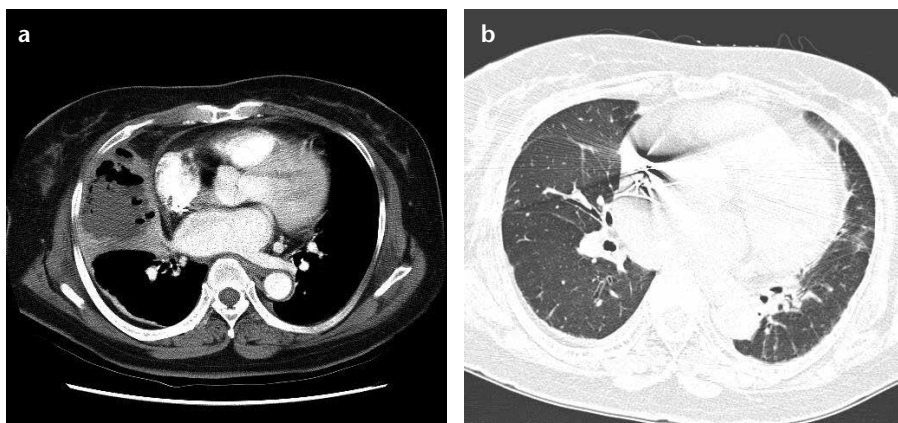


Figure 4. a, b. (Case 5) Pulmonary mucormycosis showing abscess formation with air-fluid level in a 73-year-old female patient with diabetes mellitus. Initial chest CT (a) shows dense consolidation with internal air-fluid level in the right middle lobe of the lung, representing the internal necrosis and abscess formation. Follow-up CT taken two years later (b) demonstrates no substantial residual lesions except for mild fibrosis in the right middle lobe.

tiolate pulmonary mucormycosis from invasive aspergillosis based on only CT features. Along with typical CT findings, clinical symptoms such as facial pain due to sinonasal mucormycosis, risk factors such as DM, and negative results on serum aspergillus antigen tests may facilitate the differentiation of pulmonary mucormycosis.

In our study, most patients with pulmonary mucormycosis had consistent sequential morphologic changes over follow-ups, although not all cases demonstrated the same morphologic features at the same time point. After the initial image finding of the CT halo or reversed-halo sign, pulmonary lesions tended to have internal necro-

sis; three patients with a mass or masses with the CT halo sign on initial CT had a decreased surrounding halo followed by central necrosis. In addition, one patient with a mass with the reversed-halo sign on initial CT had central necrosis. These sequential morphological changes of pulmonary mucormycosis have not yet been reported. In a previous study of 32 cases of pulmonary mucormycosis (3), the authors were not able to evaluate these sequential morphological changes as there were no follow-up CT examinations in their study. Although it is not possible to definitively correlate the sequential imaging features of pulmonary mucormycosis with their corresponding pathologic changes at each stage of the disease, we may be able to suggest which pathologic findings are related to the sequential morphological changes in follow-up CT images (Fig. 5). The halo or reversed-halo sign is typically caused by hemorrhage or infarction due to the angio-invasion of pulmonary mucormycosis, which may progress into organizing pneumonia with granulation tissue formation from the periphery of the lesion. Thereafter, internal necrosis can occur within the mass or masses. This sequential change is similar to the pathologic changes of invasive pulmonary aspergillosis. Initially, the CT halo sign appears as a fluffy mass and/or nodules caused by hemorrhagic infarction, which then enlarge and subsequently progress to cavitations or abscesses by necrosis prior to the air-crescent sign that can be seen during the recovery stage (13, 14). The air crescent sign may also be present in mucormycosis; however, this was not noted in our study (13). We believe

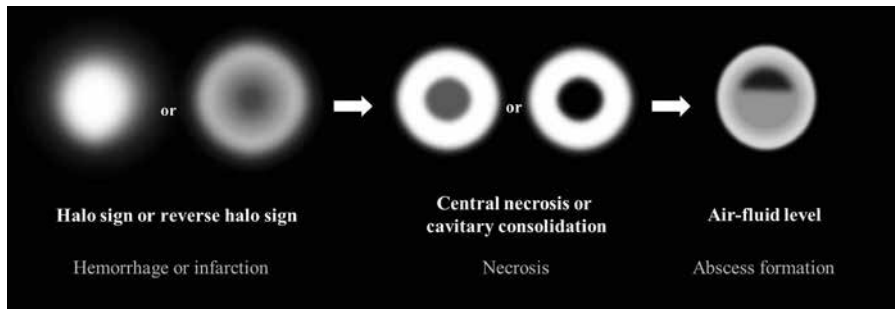


Figure 5. Schematic suggestion of sequential morphological and pathologic changes of pulmonary mucormycosis. Initially, the halo sign on CT which represents focal consolidation with adjacent ground-glass opacity, develops due to hemorrhage caused by the angioinvasive characteristics of mucormycosis. Thereafter, the reversed-halo sign may be seen. After disease progression, internal infarction causes central ground-glass opacity with peripheral consolidation. Necrotic or cavitory consolidation or masses may develop due to necrosis followed by abscess formation with an internal air-fluid line.

that these initial and sequential CT findings of pulmonary mucormycosis may facilitate diagnosis and staging of this disease. Furthermore, the change in lesion size may help to determine treatment efficacy on follow-up images. All four recovered cases showed a decrease in lesion size on follow-up CT examinations. In the expired patient, however, necrotic consolidation persistently increased in size during follow-up despite antifungal medication.

There were several limitations to the current study. First, this was a retrospective study of a small population due to the rarity of pulmonary mucormycosis. We hope that further studies will be performed in a larger number of patients with a multicenter, prospective design. Second, there may have been verification bias as we included only pathologically confirmed cases with chest CT images. Thus, we may have included only severe pulmonary mucormycosis that needed aggressive diagnostic work-ups. Third, we were not able to correlate the CT features

with the pathologic findings in each stage of each case. However, we can still conclude that pulmonary mucormycosis tends to manifest as a mass or masses with the halo or reversed-halo sign on initial CT, followed by a decreased extent of surrounding GGOs and internal necrosis during follow-up.

Acknowledgement

This research was supported by Basic Science Research Program through the National Research Foundation of Korea (NRF) funded by the Ministry of Education, Science, and Technology (grant number, 2011-0022379).

Conflict of interest disclosure

The authors declared no conflicts of interest.

References

1. Parfrey NA. Improved diagnosis and prognosis of mucormycosis. A clinicopathologic study of 33 cases. *Medicine (Baltimore)* 1986; 65:113–123. [\[CrossRef\]](#)
2. Rinaldi MG. Zygomycosis. *Infect Dis Clin North Am* 1989; 3:19–41.
3. McAdams HP, Rosado de Christenson M, Strollo DC, Patz EF Jr. Pulmonary mucormycosis: radiologic findings in 32 cases. *Am J Roentgenol* 1997; 168:1541–1548. [\[CrossRef\]](#)

4. Spellberg B, Edwards J Jr, Ibrahim A. Novel perspectives on mucormycosis: pathophysiology, presentation, and management. *Clin Microbiol Rev* 2005; 18:556–569. [\[CrossRef\]](#)
5. Horger M, Hebart H, Schimmel H, et al. Disseminated mucormycosis in haematological patients: CT and MRI findings with pathological correlation. *Br J Radiol* 2006; 79:e88–95. [\[CrossRef\]](#)
6. Jamadar DA, Kazerooni EA, Daly BD, White CS, Gross BH. Pulmonary zygomycosis: CT appearance. *J Comput Assist Tomogr* 1995; 19:733–738. [\[CrossRef\]](#)
7. Chung JH, Godwin JD, Chien JW, Pipavath SJ. Case 160: Pulmonary mucormycosis. *Radiology* 2010; 256:667–670. [\[CrossRef\]](#)
8. Hansell DM, Bankier AA, MacMahon H, McLoud TC, Muller NL, Remy J. Fleischner Society: glossary of terms for thoracic imaging. *Radiology* 2008; 246:697–722. [\[CrossRef\]](#)
9. Bigby TD, Serota ML, Tierney LM Jr, Matthay MA. Clinical spectrum of pulmonary mucormycosis. *Chest* 1986; 89:435–439. [\[CrossRef\]](#)
10. Lehrer RI HD, Sypherd PS. Mucormycosis. *Ann Intern Med* 1980; 93:93–108. [\[CrossRef\]](#)
11. Kim N, Barrie J, Raymond G. Residents' corner. Answer to case of the month #87: Pulmonary mucormycosis with angioinvasion of the left subclavian artery. *Can Assoc Radiol J* 2002; 53:312–314.
12. Gasparetto EL, Escuissato DL, Davaus T, et al. Reversed halo sign in pulmonary paracoccidioidomycosis. *AJR* 2005; 184:1932–1934. [\[CrossRef\]](#)
13. Aquino SL, Kee ST, Warnock ML, Gamsu G. Pulmonary aspergillosis: imaging findings with pathologic correlation. *AJR* 1994; 163:811–815. [\[CrossRef\]](#)
14. Franquet T, Müller NL, Giménez A, Gueembe P, de La Torre J, Bagué S. Spectrum of pulmonary aspergillosis: histologic, clinical, and radiologic findings. *Radiographics* 2001; 21:825–837.